NASA TN D-280

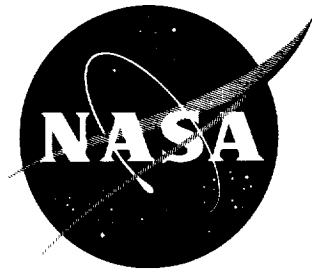

TECHNICAL NOTE

D-280

FLIGHT MEASUREMENT OF WALL-PRESSURE FLUCTUATIONS AND BOUNDARY-LAYER TURBULENCE

By Harold R. Mull and Joseph S. Algranti

Lewis Research Center
Cleveland, Ohio

NATIONAL AERONAUTICS AND SPACE ADMINISTRATION

WASHINGTON

October 1960

NATIONAL AERONAUTICS AND SPACE ADMINISTRATION

TECHNICAL NOTE D-280

FLIGHT MEASUREMENT OF WALL-PRESSURE FLUCTUATIONS AND BOUNDARY-LAYER TURBULENCE

By Harold R. Mull and Joseph S. Algranti

SUMMARY

The results are presented for a flight test program using a fighter type jet aircraft flying at pressure altitudes of 10,000, 20,000, and 30,000 feet at Mach numbers from 0.3 to 0.8. Specially designed apparatus was used to measure and record the output of microphones and hot-wire anemometers mounted on the forward-fuselage section and wing of the airplane. Mean-velocity profiles in the boundary layers were obtained from total-pressure measurements.

The ratio of the root-mean-square fluctuating wall pressure to the free-stream dynamic pressure is presented as a function of Reynolds number and Mach number. The longitudinal component of the turbulent-velocity fluctuations was measured, and the turbulence-intensity profiles are presented for the wing and forward-fuselage section.

In general, the results are in agreement with wind-tunnel measurements which have been reported in the literature. For example, the variation of $\sqrt{\overline{p^2}}/q$ ($\sqrt{\overline{p^2}}$ is the root mean square of the wall-pressure fluctuation, and q is the free-stream dynamic pressure) with Reynolds number was found to be essentially constant for the forward-fuselage-section boundary layer, while variations at the wing station were probably unduly affected by the microphone diameter (5/8 in.), which was large compared with the boundary-layer thickness.

INTRODUCTION

The problem of aircraft noise has two facets: one from the viewpoint of the passengers within the airplane, and the other from the viewpoint of the people on the ground in the neighborhood of the airport where planes are arriving and departing. As aircraft speeds increase and as jet-powered planes come into use, more of the inside noise originates from the air flowing along the fuselage and less from

the powerplant and vibration. In the speed range of the modern jet transport (high subsonic) boundary-layer noise may be the dominant source of annoyance to crew and passengers. Boundary-layer noise has been the subject of several theoretical studies on the transmission of sound through the skin of aircraft and the resulting reverberent buildup in the interior (refs. 1 to 5).

Application of the results of these analyses has been hampered by inadequate data on the magnitude and spectra of the fluctuating pressures on the outside of the skin due to the presence of the turbulent boundary layer. Flight information is very limited (see ref. 6), and wind-tunnel investigations have not covered a wide range of conditions. Experimental studies have been done on boundary-layer noise in a small pipe with a flexible wall (refs. 7 and 8), in a wind tunnel (ref. 9), and in boundary layers formed as water flows along a model (ref. 10).

In order to supply more information the flight tests described in this report were undertaken. Wall-pressure fluctuations, turbulent-velocity fluctuations, and mean-velocity profiles were measured in flight as part of the aerodynamic noise program of the NASA Lewis Research Center.

INSTRUMENTATION

The boundary-layer measurements described in this report were taken at a station on the forward-fuselage section of an F-94 jet fighter aircraft and on the wing. These locations were selected because they permitted installation of the measuring probes and controls in the airplane structure. The wall-pressure fluctuations were measured with a microphone mounted flush with the airplane skin at two locations: on the forward-fuselage section 5.5 feet from the stagnation point at the nose, and on the wing 2.8 feet from the leading edge at 42 percent of chord. A flight model hot-wire anemometer was used to measure the longitudinal-turbulent-velocity fluctuations through the boundary layer, while the mean-velocity profiles in the boundary layer were measured with a total-pressure probe or a total-pressure rake. Photographs of the measuring stations with the various probes mounted in place are shown in figures 1 and 2. A block diagram of the instrumentation is given in figure 3.

Two methods were used to install the two microphones for these experiments. For the forward-fuselage section the microphone was machined from a single piece of metal so that the diaphragm was the top surface of the capsule. In this way the shape could be made to approximate the shape of the skin on the forward-fuselage section of the plane, and thus no unusual irregularities occurred at the face of the microphone. The surface of the skin was made smooth by filling in all screw slots and other indentations with appropriate fillers and removing all projections. The microphone had a diameter of 5/8 inch, and its frequency response was ± 3 decibels from 50 to 25,000 cycles per second.

For the wing location a sintered bronze material was machined and cut to fit the location chosen on the wing. The condenser-type microphone was mounted inside the wing just below this sintered plug (5/8 in. diam.). Extensive tests show that the basic frequency response of the microphone (±3 db from 10 to 15,000 cps) was not seriously deteriorated by the presence of the sintered material. A standard power supply was used for the microphones.

The mean-velocity profiles in the boundary layer were measured by means of total-pressure probes. In the case of the nose installation a rake was fabricated which consisted of nine tubes 1/32 inch in diameter arranged to give an adequate representation of the boundary layer developed on the nose of the plane. The pressures monitored by the rake were switched successively by three-way solenoid valves to a single differential pressure gage. The electrical output of the pressure transducer was recorded by a self-balancing-potentiometer chart recorder. These signals together with the calibrations could be used to obtain the velocity profile within the boundary layer.

For the thinner boundary layer at the wing station a single total-pressure probe was driven from the surface of the wing well into the free-stream flow over the wing. This probe was actuated by a screw-type actuator which also drove the hot-wire probe. The electrical signals from the pressure transducer controlled the frequency of a telemeter subcarrier oscillator. These signals were then recorded on magnetic tape.

The electrical signals from the hot-wire probe were controlled and compensated for frequency response by a specially built flight model of a self-exciting alternating-current constant-temperature hot-wire anemometer (ref. 11, fig. 3, and fig. 4 of this report). This anemometer had a cutoff frequency response of approximately 7000 cycles per second and used a 0.0005-inch-diameter (1/2-mil) tungsten wire. The electrical signals from the hot-wire anemometer were recorded on a flight type magnetic tape recorder (fig. 5). This recorder, which could accept seven simultaneous signal channels, was also used to record the probe position and the microphone signals. One channel was used for voice recording of the flight conditions and certain other data such as the root mean square of the hot-wire voltage and the average value of the a-c carrier which heated the wire. These two voltages were indicated by meters mounted in the cockpit, and the voice recordings of their magnitude were used to calibrate the hot-wire voltage signals recorded on the tape. The microphones were calibrated in the usual way by means of a standard acoustic source driven by a transistor oscillator which gave sine wave calibrations at 400 and/or 1000 cycles per second.

EXPERIMENTAL PROCEDURE

Data Acquisition

Flight data were taken at pressure altitudes of 10,000, 20,000, and 30,000 feet and over a range of Mach numbers of 0.3 to 0.8. Prior to each data flight the pressure transducers were calibrated. Several signals of known frequency and voltage level were recorded on magnetic tape. These signals provided a means for checking the response of the playback and record mechanism as well for setting playback levels. Zero levels were also checked and recorded so that any frequency shift of the telemeter subcarrier oscillator could be detected.

The microphone was calibrated prior to each flight by means of the calibrator mentioned in the section INSTRUMENTATION. The hot-wire instrumentation was calibrated at frequent intervals, and the hot-wire probe itself was calibrated before each flight.

The flight plan for taking the data was to climb to the desired altitude and stabilize the aircraft at the desired speed. At this time a recording was made of the wall-pressure fluctuations, the boundary-layer velocity fluctuations at a given hot-wire probe position, and the total-pressure measurements. The flight test conditions were voice-recorded. Then a new condition was established, and the recordings were repeated.

Data Reduction

The recordings of the data were used to obtain the following: the mean-velocity profiles in the boundary layer, the turbulence-intensity profiles, the spectra of turbulence, the wall-pressure fluctuations, and their spectra.

The mean-velocity profiles were calculated from measurements of aircraft total temperature, probe total pressure, and skin static pressure. The turbulence intensity was computed using the methods of reference 12, and the spectra of the turbulence in the boundary layer were obtained by the methods of reference 13.

RESULTS AND DISCUSSION

The results of the wall-pressure measurements are plotted in figures 6 and 7. In these plots the ratio of the root-mean-square fluctuating wall pressure to the free-stream dynamic pressure is plotted against Reynolds number and Mach number. Because of the difficulties involved in calibration, the effect of altitude on microphone sensitivity was not

evaluated. An estimated reduction of 2 decibels in the readings at 30,000 feet and of 1 decibel at 20,000 feet was used in compiling the data for the two figures (see ref. 14).

The magnitudes of the ratio of root-mean-square pressures to dynamic pressure ($\sqrt{\overline{p^2}}/q$) on the forward-fuselage section at the lower Reynolds numbers were close to those predicted for a flat plate in reference 1 (0.006) and were approximately the value observed in reference 8 in a 1-inch pipe.

The values of $\sqrt{\overline{p^2}}/q$ as measured are influenced by the size of the microphone as compared with the boundary-layer thickness. From the microphone diameter (d = 5/8 in.) and the 1/7 power law shown in figure 8 (a value of $\delta^*/\delta = 1/8$) a value of $d/\delta = 6.25$ is calculated. An extrapolation of figure 5 of reference 8 (see fig. 9) indicated $\sqrt{\overline{p^2}}/q$ values of 4×10^{-3}, which compares quite well with the measured value. (Symbols are defined in the appendix.)

The magnitude of $\sqrt{\overline{p^2}}/q$ was much less on the wing than on the forward-fuselage section. This difference in magnitude was also noted with the turbulence intensities, which are discussed later. The two points (taken on the wing at 30,000 ft) that lie well above the others in figure 6 were at local Mach numbers of 0.86 and 0.9. The turbulence intensities also show a sharp rise in this region, indicating possible onset of local shock patterns. This was observed at the high speeds at the 20,000-foot altitude with the signal being too erratic to measure.

The reasons for the lower fluctuating pressures at the wing station are not understood at this time. For the wing station d/δ^* turns out to be about 15 to 20. Such a large extrapolation of the data of reference 8 (fig. 9) is hardly justified, but it does indicate that the low values of $\sqrt{\overline{p^2}}/q$ are at least partly caused by microphone size as compared with boundary-layer thickness. Other contributing factors are the lower turbulence intensity and smaller boundary-layer thickness as compared with the forward-fuselage section, as is discussed later. The run from the stagnation point on the nose was 5.5 feet, and it was found that static-pressure recovery was nearly complete. In contrast, the location of the station on the wing was near the minimum-static-pressure point (2.8 ft from the leading edge or 42 percent of the chord). The boundary-layer turbulence was thus growing along a favorable pressure gradient.

Figure 7 illustrates the variation of $\sqrt{\overline{p^2}}/q$ with Mach number for the forward-fuselage-section and wing stations. As shown by the curve the total variation at the forward-fuselage station was only a little more than ±1 decibel for all altitudes and Mach numbers. But at the wing the result is different. The curves show that the altitude is an important parameter and that the total variation with Mach number is nearly an order of magnitude (i.e., 20 db).

The boundary-layer-velocity profiles showed the effect of this difference in history. The profiles taken at the forward-fuselage station have a typical 1/7 power law shape (fig. 8), while that of the wing was more nearly 1/5 or 1/6 (fig. 10). In figure 11 the boundary-layer profiles for constant Mach number at the wing station illustrate the effect of altitude on the boundary layer. As might be expected, there is only a slight effect.

Since instrumentation used in this experiment measured only the longitudinal-velocity fluctuations, the discussion of turbulent velocity fluctuations is necessarily limited to that extent. Figures 12 and 13 show the turbulent-velocity profiles in the boundary layer at the three pressure altitudes at the nose and wing stations, respectively. At the nose station (fig. 12) a typical increase in turbulence intensity occurs as the distance from the wall is decreased until a reversal occurs at distances of about 0.05 inch from the wall. The scatter in the data is rather large, but considering the difficulty involved in obtaining data, it shows a trend of increased intensity with decreasing Mach number. This variation is to be expected.

For the wing station (fig. 13) the results are similar except that the boundary layer was much thinner at the wing station than on the nose of the plane. In figure 13(a) the data for a 10,000-foot pressure altitude and a local Mach number of 0.758 show the effect of buffeting or possibly of local shocks.

The spectral analysis of the wall-pressure fluctuations and the boundary-layer longitudinal-velocity fluctuations is given in figures 14 to 16. In figure 14, the spectrum levels referred to the overall level for the nose station and the three pressure altitudes of 10,000, 20,000, and 30,000 feet are given for two Mach numbers. There is little difference in the three curves except for more scatter in the low-frequency bands at the highest altitude. The spectra are very flat with only the slight indication of a peak in the neighborhood of 800 to 900 cycles per second. The Mach number likewise has little effect on the wall-pressure fluctuations at the nose station. For the wing station the spectra for a 10,000-foot pressure altitude and Mach numbers 0.3 and 0.6 are presented. At a Mach number of 0.3 the spectrum is flat with a resonant peak at 5000 cycles per second, while at a Mach number of 0.6 the variation and scatter may be the result of buffeting at this speed and altitude.

Figure 15 shows the spectral analysis of the wall-pressure fluctuations at a pressure altitude of 10,000 feet at the forward-fuselage and wing stations while the airplane speed was varied through a series of Mach numbers. The curves for both stations show considerable scatter at the highest subsonic Mach number (0.65 for the forward-fuselage section and 0.55 for the wing), and the spectrum level begins to fall off after 250 cycles per second. For the other Mach numbers there is evidence that

the spectrum level is somewhat greater for the larger Mach numbers, a flat distribution being the major characteristic of the noise. There is only a slight tendency to peak at about 200 to 300 cycles per second for this range of Mach numbers.

The spectral distribution of the longitudinal-velocity fluctuations at four positions within the boundary layer is given in figure 16. The curves show a slight tendency to peak at approximately 400 cycles per second with an indication of more energy in the velocity fluctuations as the distance from the surface is increased. There is insufficient evidence to show the reversal in turbulence intensity that is shown in figure 12.

CONCLUDING REMARKS

Measurements of wall-pressure fluctuations and boundary-layer turbulence taken in flight tests of a fighter type jet aircraft have shown:

1. The wall-pressure fluctuations measured on the forward-fuselage section of the aircraft agree well with an extrapolation of boundary-layer data obtained in the laboratory when the relative size of the microphone as compared with the boundary-layer thickness is the same. Similar extrapolations indicate that a possible explanation for the low measured values of $\sqrt{\overline{p^2}}/q$ for the wing station (where $\sqrt{\overline{p^2}}$ is the root mean square of the wall-pressure fluctuations, and q is free-stream dynamic pressure) is the large size of the microphone compared with the thickness of the boundary layer.

2. Mean-velocity profiles on the forward-fuselage section conform to a 1/7 power law, but those on the wing are perhaps of a 1/5 power law.

3. Turbulent-velocity profiles measured at the forward-fuselage and wing stations are typical of flat-plate boundary layers.

4. The spectral distributions of the wall-pressure and turbulent-velocity fluctuations in the boundary layer are quite flat with only a slight tendency to peak.

Lewis Research Center
National Aeronautics and Space Administration
Cleveland, Ohio, July 11, 1960

APPENDIX - SYMBOLS

d	microphone diameter
$\sqrt{\overline{p^2}}$	measured root-mean-square wall pressure
q	free-stream dynamic pressure
Re_x	Reynolds number, $\rho U_l x/\mu$
U	free-stream velocity
U_l	local free-stream velocity
u	fluctuating component of free-stream velocity in x-direction
u'	root mean square of fluctuating velocity, $\sqrt{\overline{u^2}}$
x	distance along surface from tip of nose of fuselage or from leading edge of wing
y	distance from airplane surface
δ	boundary-layer thickness
δ^*	$\int_0^\delta \left(1 - \frac{U}{U_l}\right) dy$
μ	coefficient of viscosity of air
ρ	air density at free-stream conditions

REFERENCES

1. Phillips, O. M.: On Aerodynamic Surface Sound. FM 2099, British ARC, Mar. 28, 1955.

2. Phillips, O. M.: On the Aerodynamic Surface Sound from a Plane Turbulent Boundary Layer. Proc. Roy. Soc. (London), ser. A, vol. 234, no. 1198, Feb. 21, 1956, pp. 327-335.

3. Corcos, G. M., and Liepmann, H. W.: On the Contribution of Turbulent Boundary Layers to the Noise Inside a Fuselage. NACA TM 1420, 1956.

4. Ribner, H. S.: Boundary-Layer-Induced Noise in the Interior of Aircraft. Rep. 37, Inst. Aerophys., Univ. Toronto, Apr. 1956.

5. Kraichnan, Robert H.: Noise Transmission from Boundary Layer Pressure Fluctuations. Jour. Acoustical Soc. Am., vol. 29, no. 1, Jan. 1957, pp. 65-80.

6. Mull, Harold R., and Algranti, Joseph S.: Preliminary Flight Survey of Aerodynamic Noise on an Airplane Wing. NACA RM E55K07, 1956.

7. Willmarth, William W.: Wall Pressure Fluctuations in a Turbulent Boundary Layer. Jour. Acoustical Soc. Am., vol. 28, no. 6, Nov. 1956, pp. 1048-1053.

8. Willmarth, W. W.: Space-Time Correlations and Spectra of Wall Pressure in a Turbulent Boundary Layer. NASA MEMO 3-17-59W, 1959.

9. Harrison, Mark: Correlations and Spectra of Pressure Fluctuations on the Wall Adjacent to a Turbulent Boundary Layer. Jour. Acoustical Soc. Am., vol. 29, no. 11, Nov. 1957, p. 1252.

10. Skudrzyk, E. J., and Haddle, G. P.: Noise Production in a Turbulent Boundary Layer by Smooth and Round Surfaces. Jour. Acoustical Soc. Am., vol. 32, no. 1, Jan. 1960, pp. 19-34.

11. Shepard, Charles E.: A Self-Excited, Alternating-Current, Constant-Temperature Hot-Wire Anemometer. NACA TN 3406, 1955.

12. Laurence, James C., and Landes, L. Gene: Auxiliary Equipment and Technique for Adapting the Constant-Temperature Hot-Wire Anemometer to Specific Problems in Air-Flow Measurements. NACA TN 2843, 1952.

13. Laurence, James C.: Intensity, Scale, and Spectra of Turbulence in a Free Subsonic Jet. NACA Rep. 1292, 1956. (Supersedes NACA TN's 3561 and 3576.)

14. Beranek, Leo L.: Acoustic Measurements. John Wiley & Sons, Inc., 1949, p. 219.

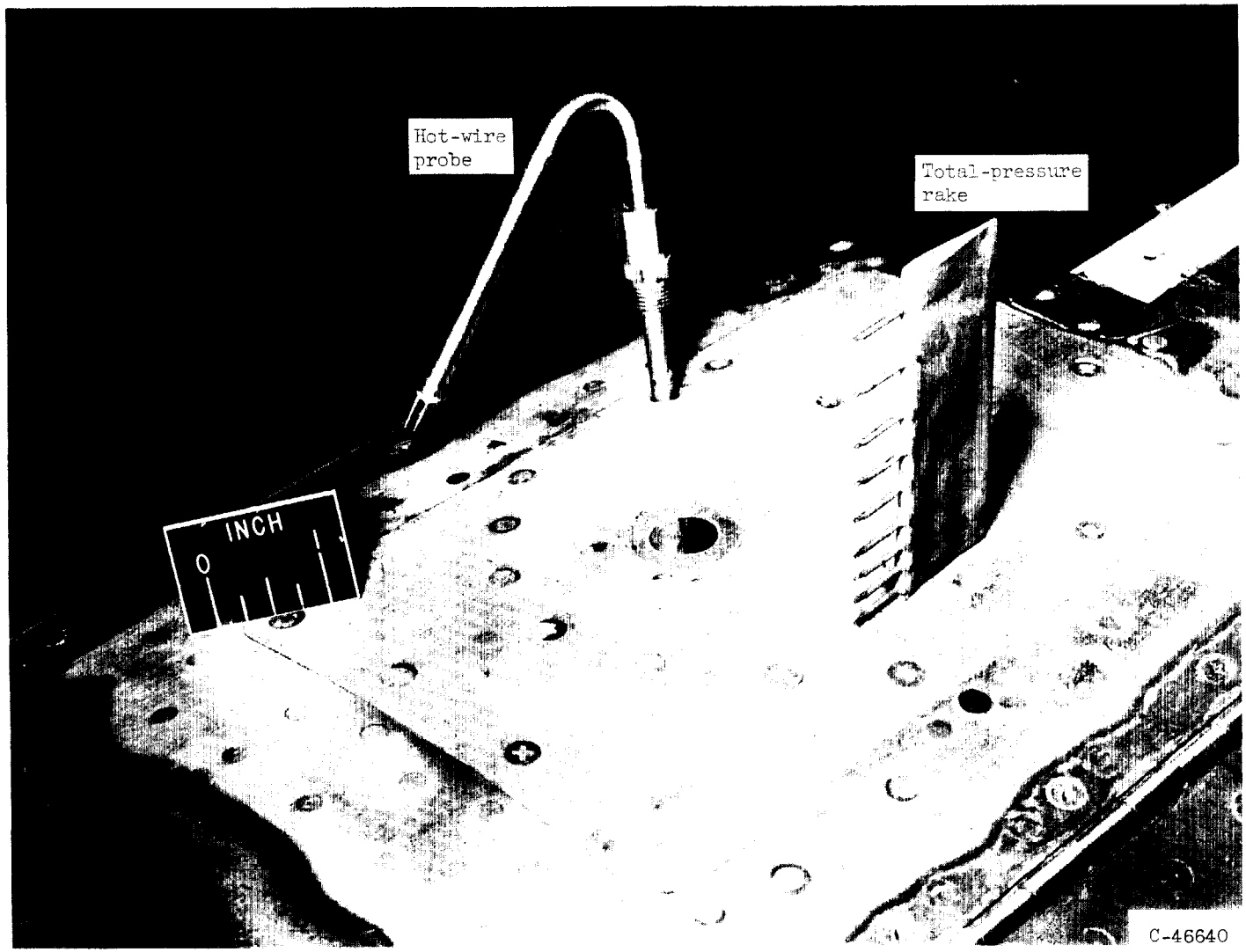

Figure 1. - Measuring station on forward fuselage section showing hot-wire probe, microphones, and total-pressure rake.

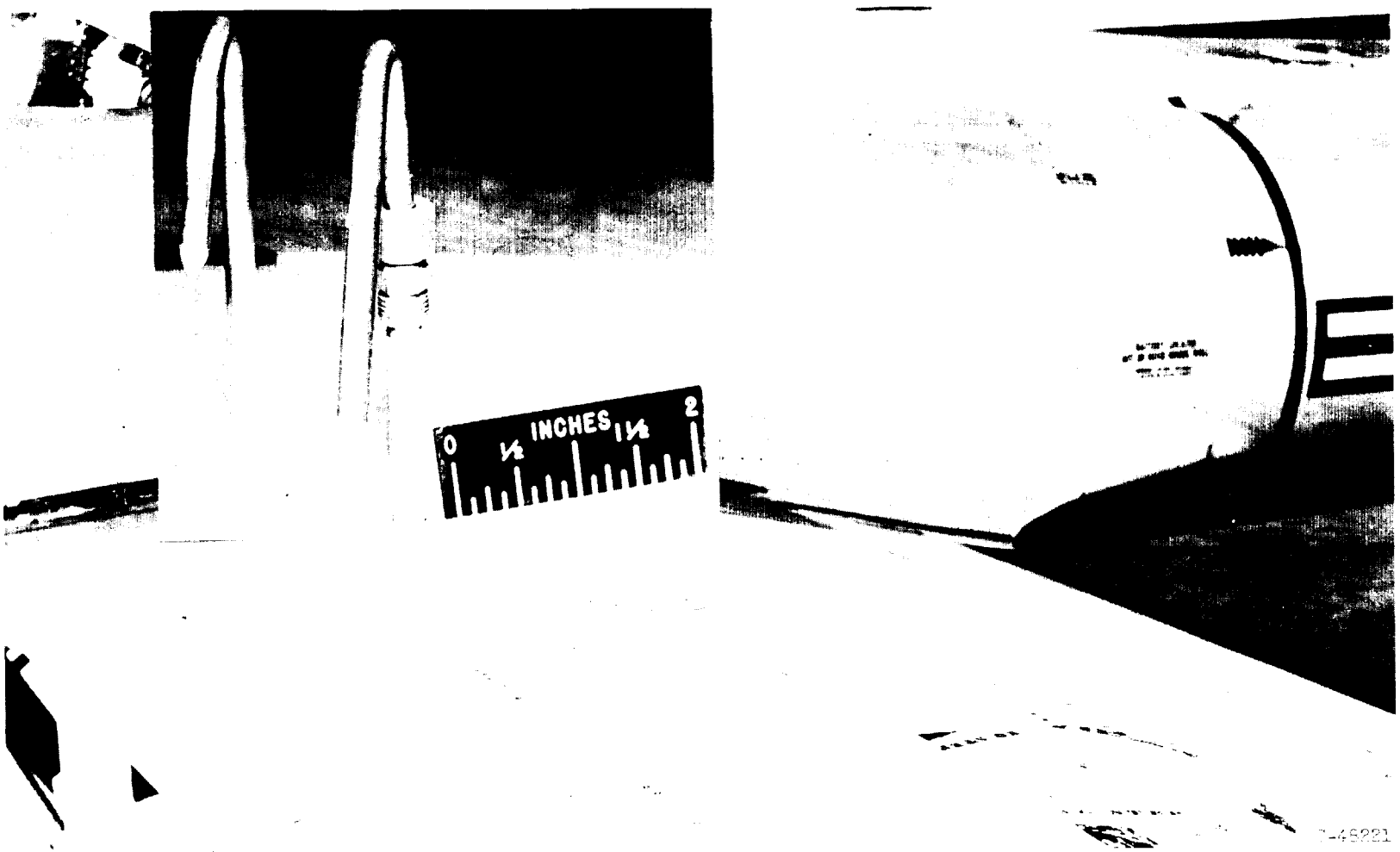

Figure 2. - Measuring station on airplane wing showing total-pressure and hot-wire probes.

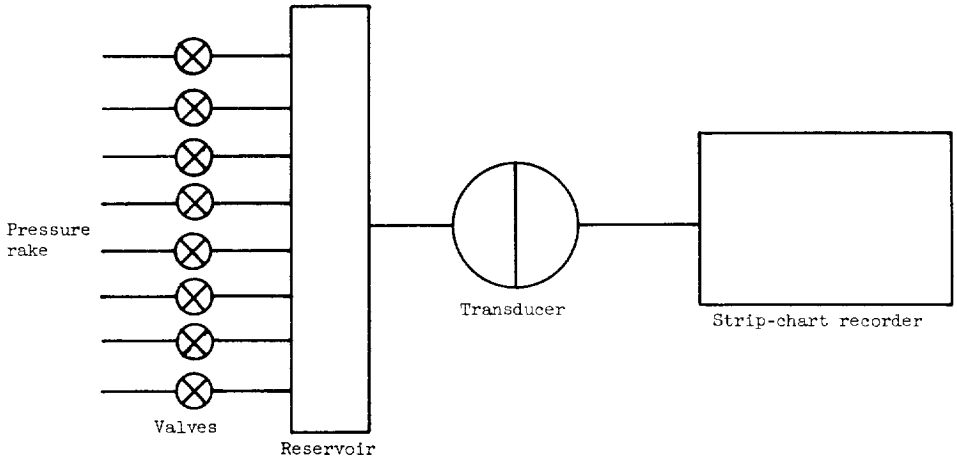

(a) Pressure recording system for forward-fuselage section.

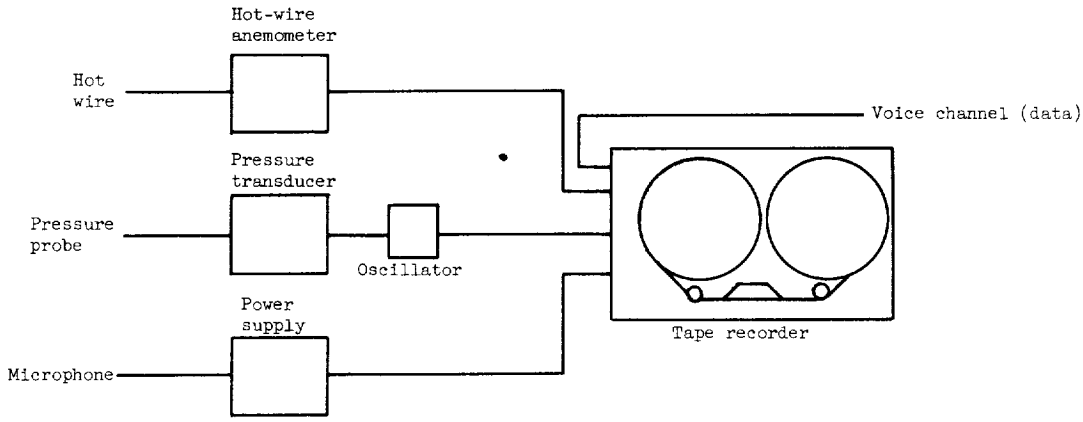

(b) Data recording system for both stations.

Figure 3. - Block diagram of instrumentation.

C-46638

Figure 4. - Hot-wire anemometer installed in airplane.

Figure 5. - Tape recorder installed in airplane.

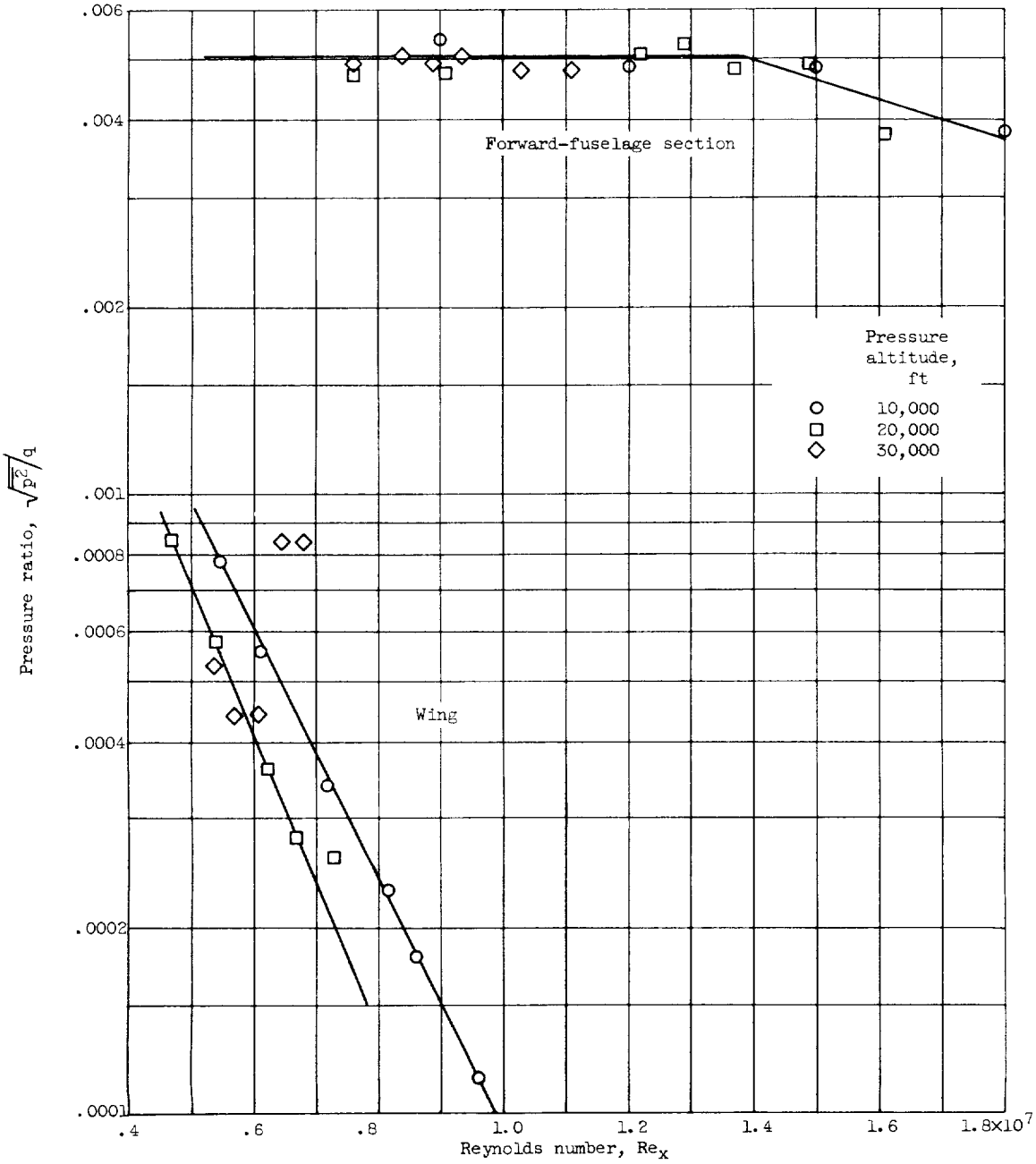

Figure 6. - Wall-pressure fluctuations as function of Reynolds number.

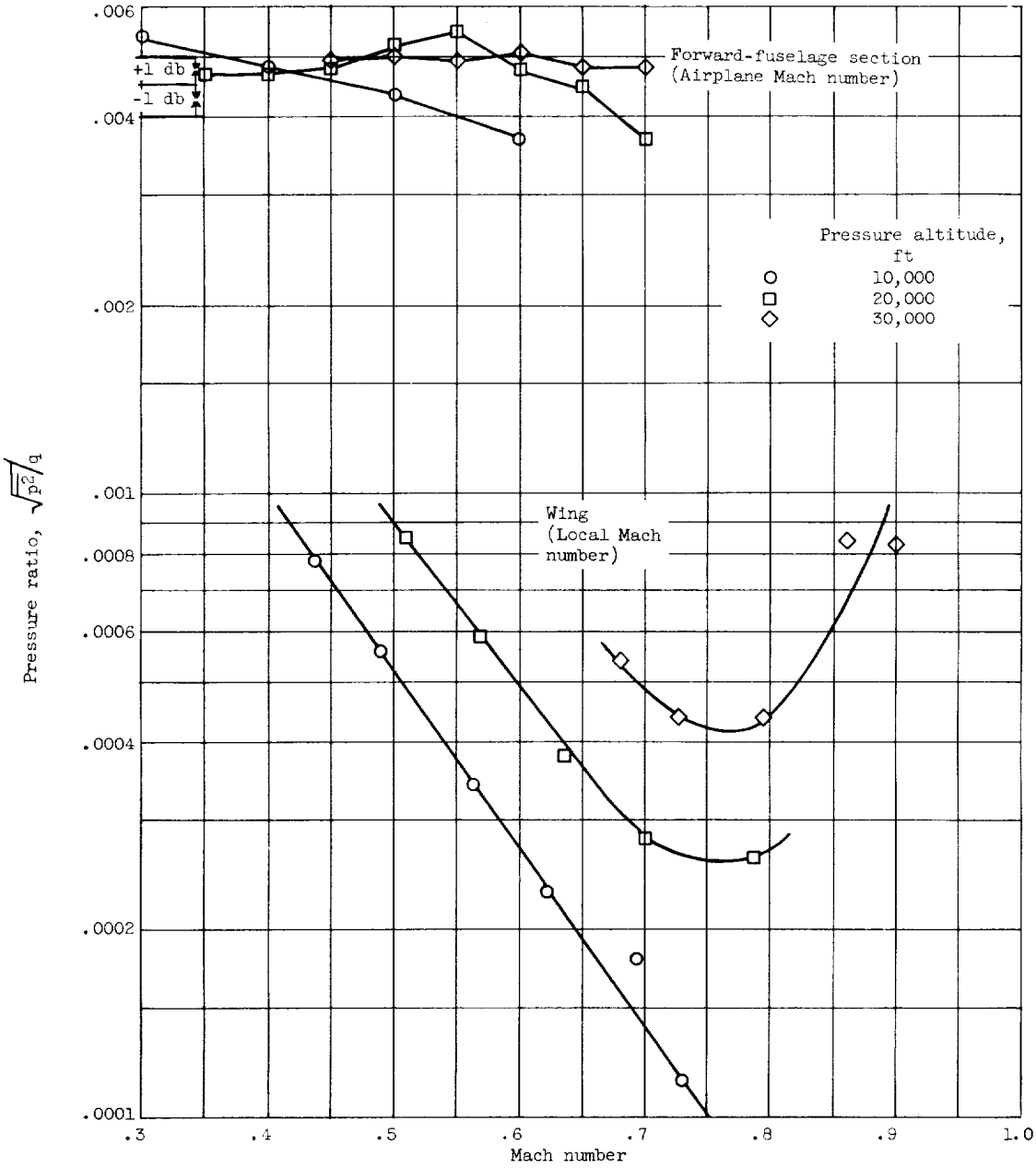

Figure 7. - Wall-pressure fluctuations as function of Mach number.

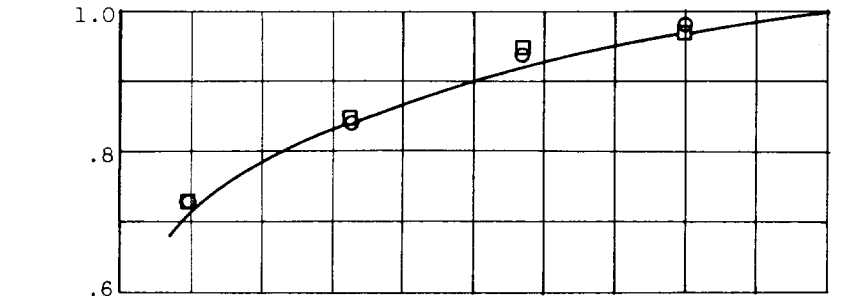

(a) Pressure altitude, 10,000 feet.

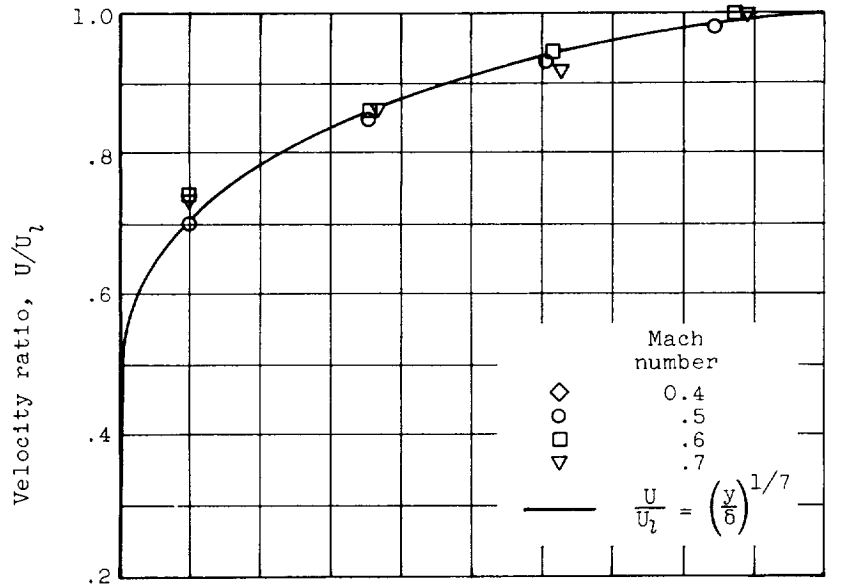

(b) Pressure altitude, 20,000 feet.

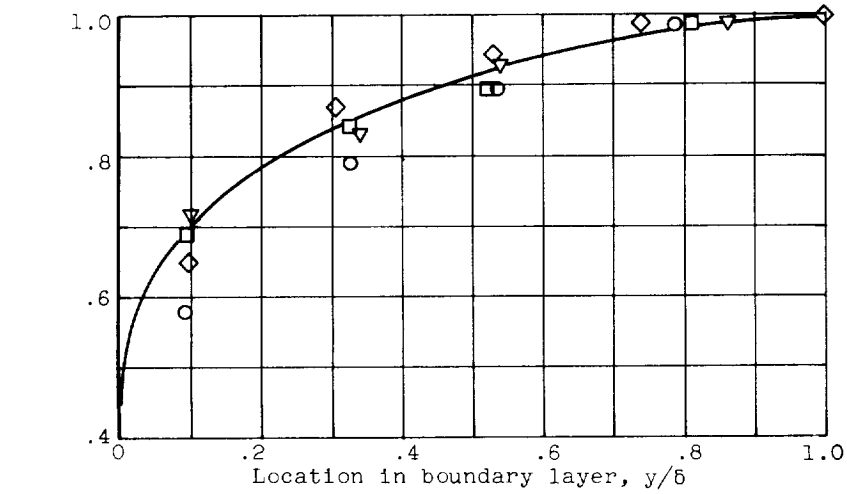

(c) Pressure altitude, 30,000 feet.

Figure 8. - Boundary-layer profile for forward-fuselage section.

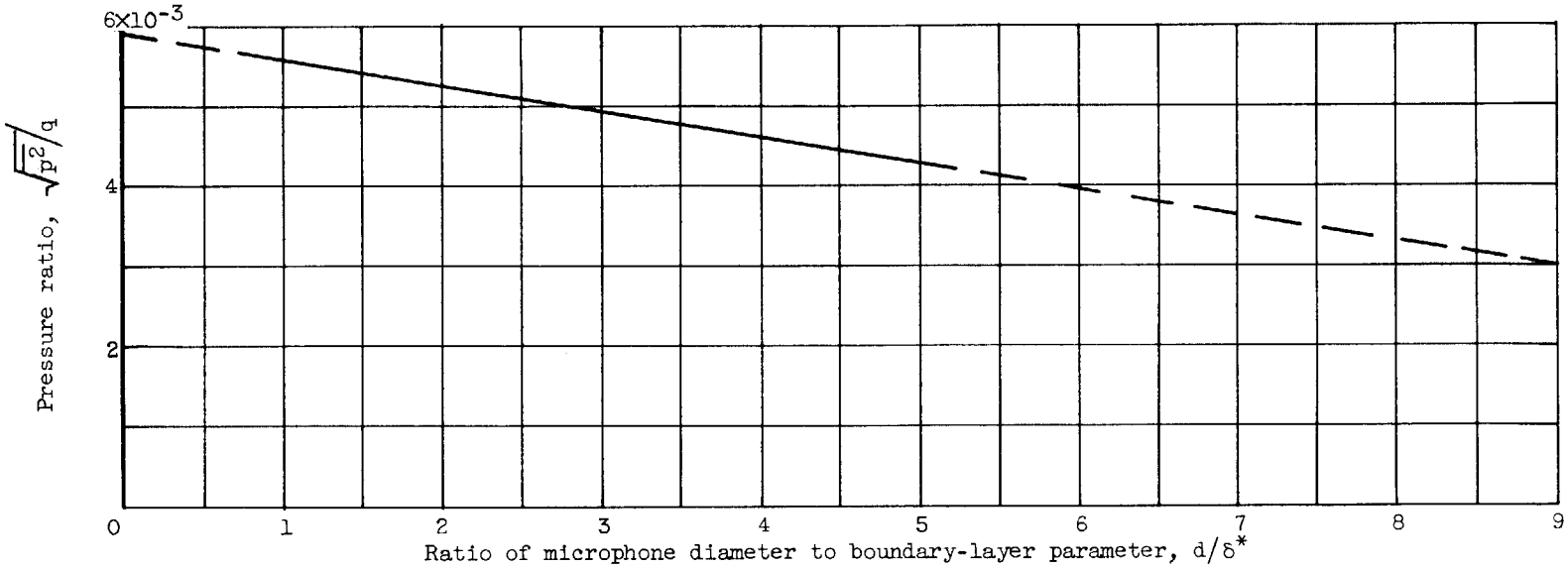

Figure 9. - Ratio of root-mean-square wall pressure to free-stream dynamic pressure in turbulent boundary layer (ref. 8, fig. 5).

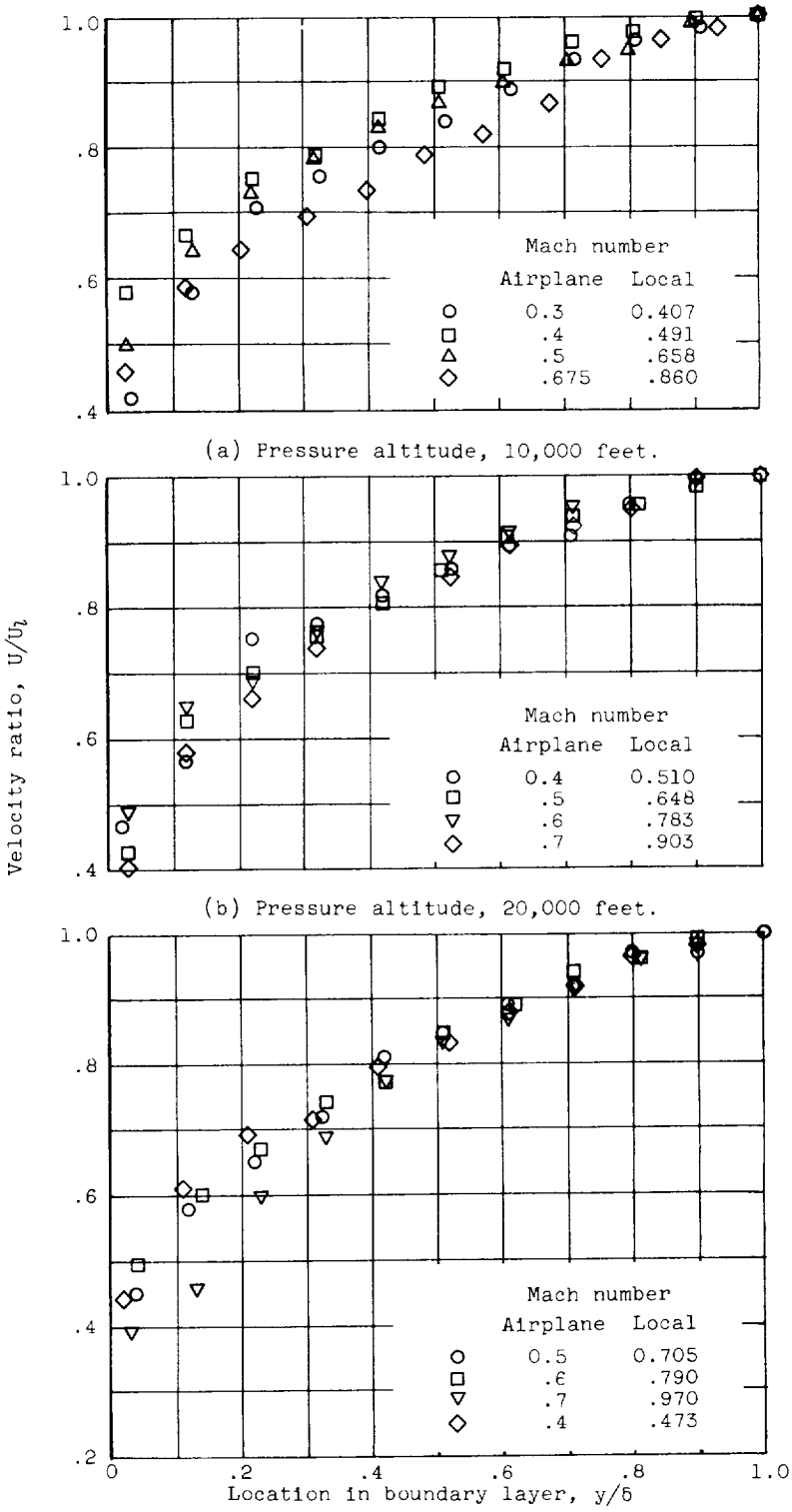

Figure 10. - Boundary-layer profiles for wing at various airplane and local Mach numbers.

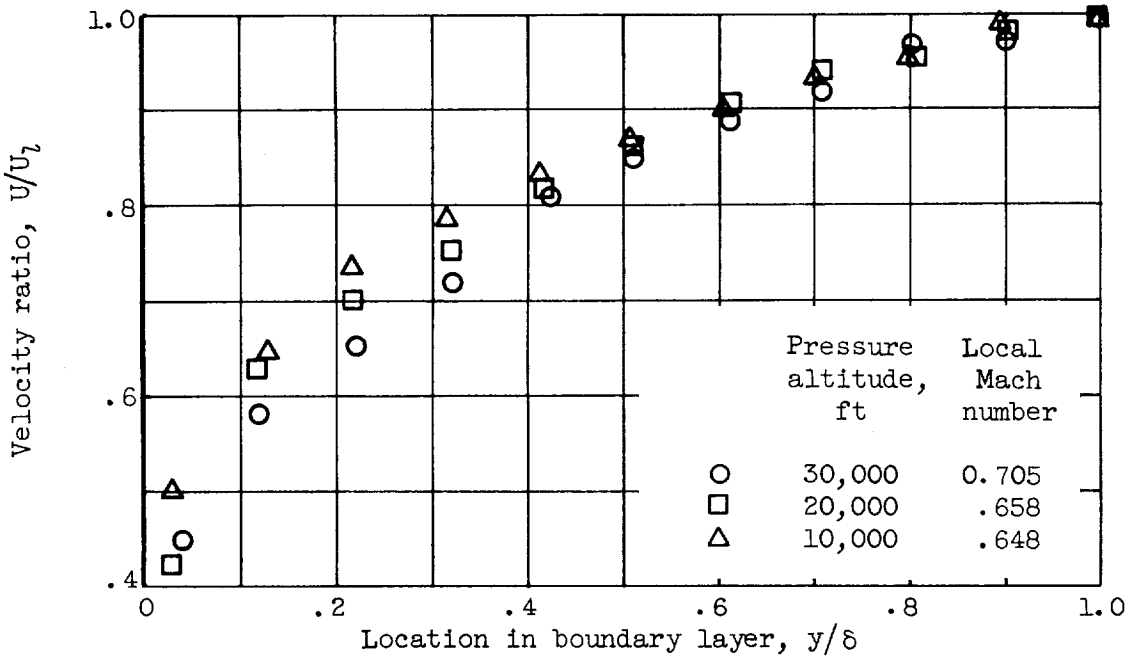

Figure 11. - Boundary-layer profile for wing at airplane Mach number of 0.5.

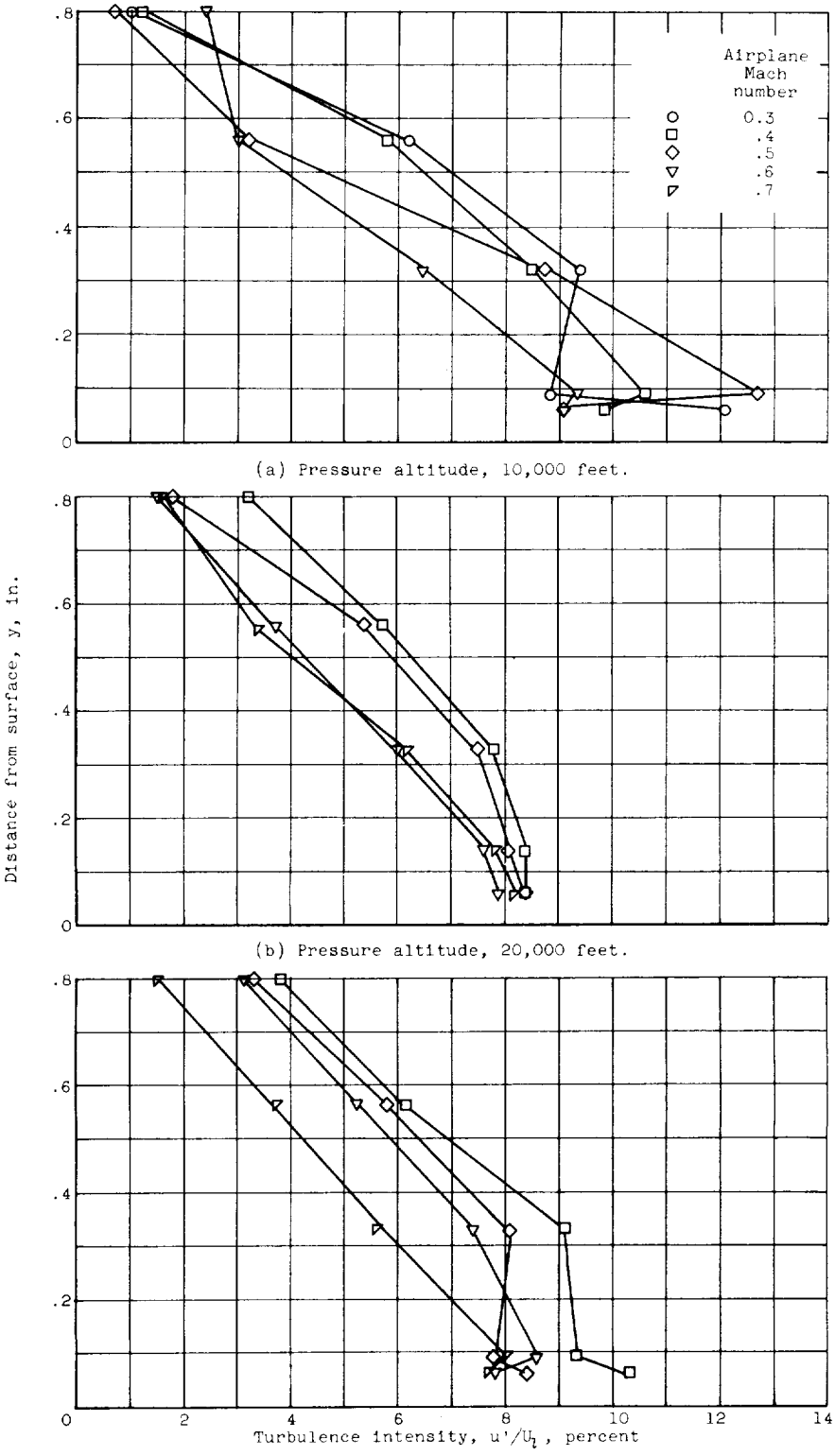

(a) Pressure altitude, 10,000 feet.

(b) Pressure altitude, 20,000 feet.

(c) Pressure altitude, 30,000 feet.

Figure 12. - Turbulent-velocity profile for forward-fuselage section.

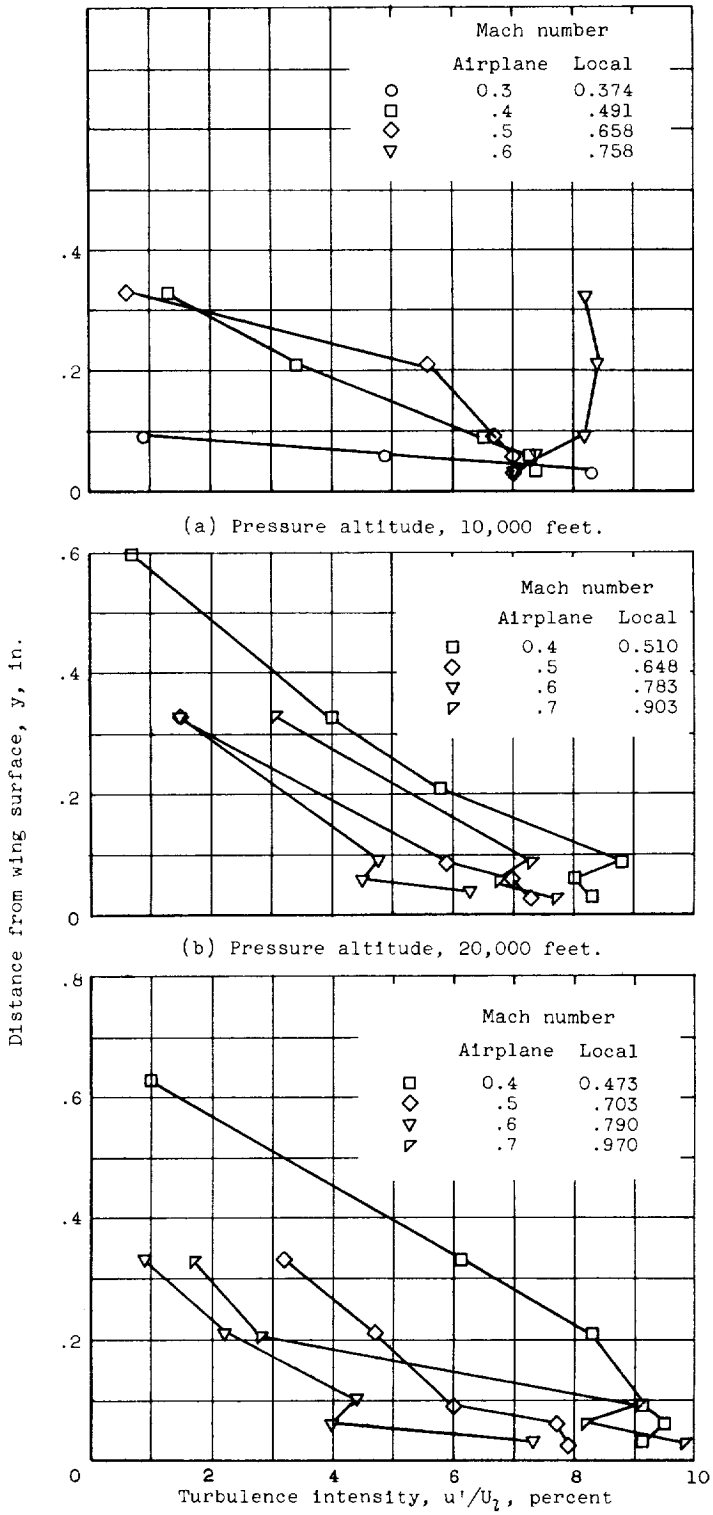

(a) Pressure altitude, 10,000 feet.

(b) Pressure altitude, 20,000 feet.

(c) Pressure altitude, 30,000 feet.

Figure 13. - Turbulent-velocity profile for wing.

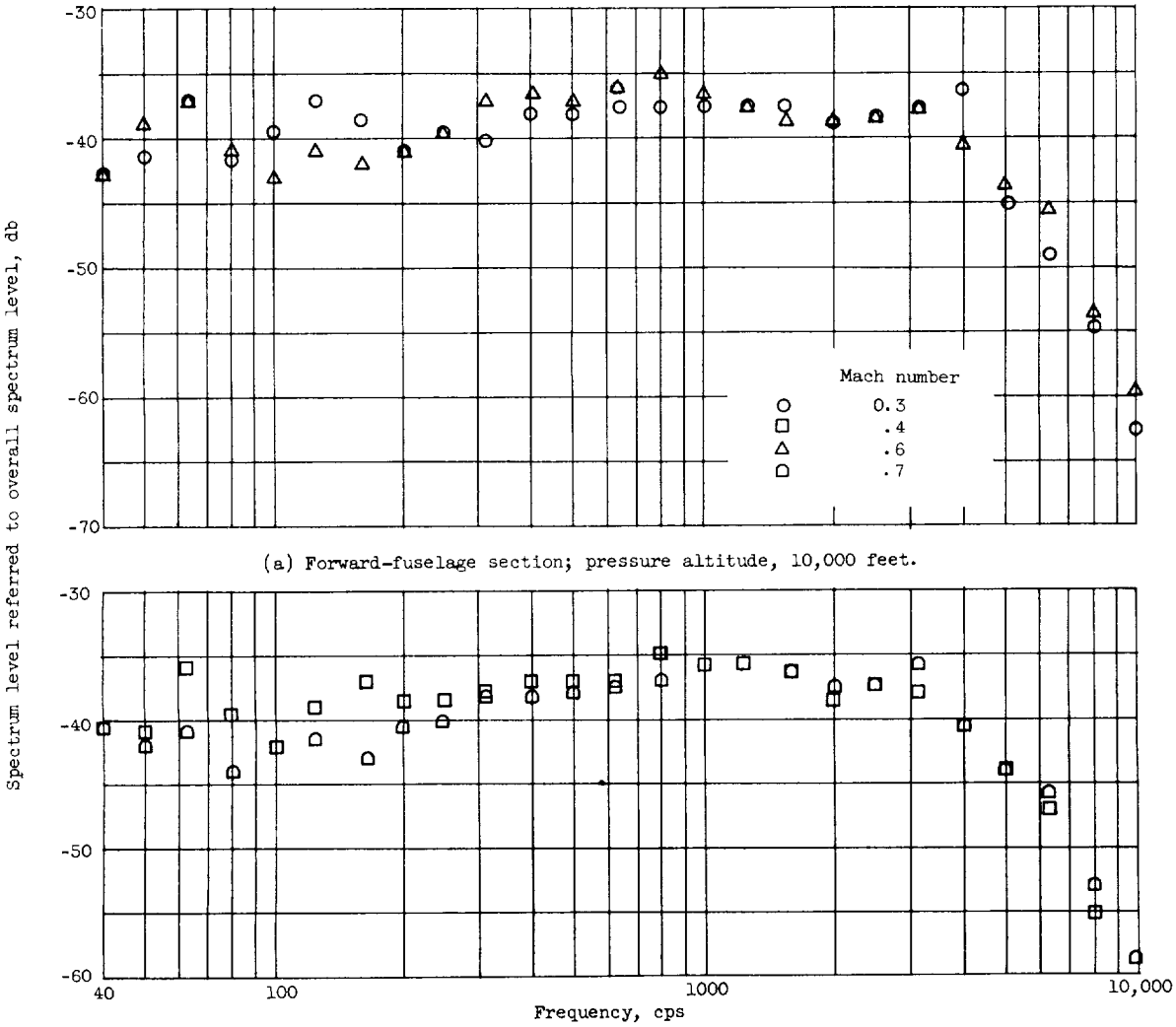

(a) Forward-fuselage section; pressure altitude, 10,000 feet.

(b) Forward-fuselage section; pressure altitude, 20,000 feet.

Figure 14. - Wall-pressure spectrum level.

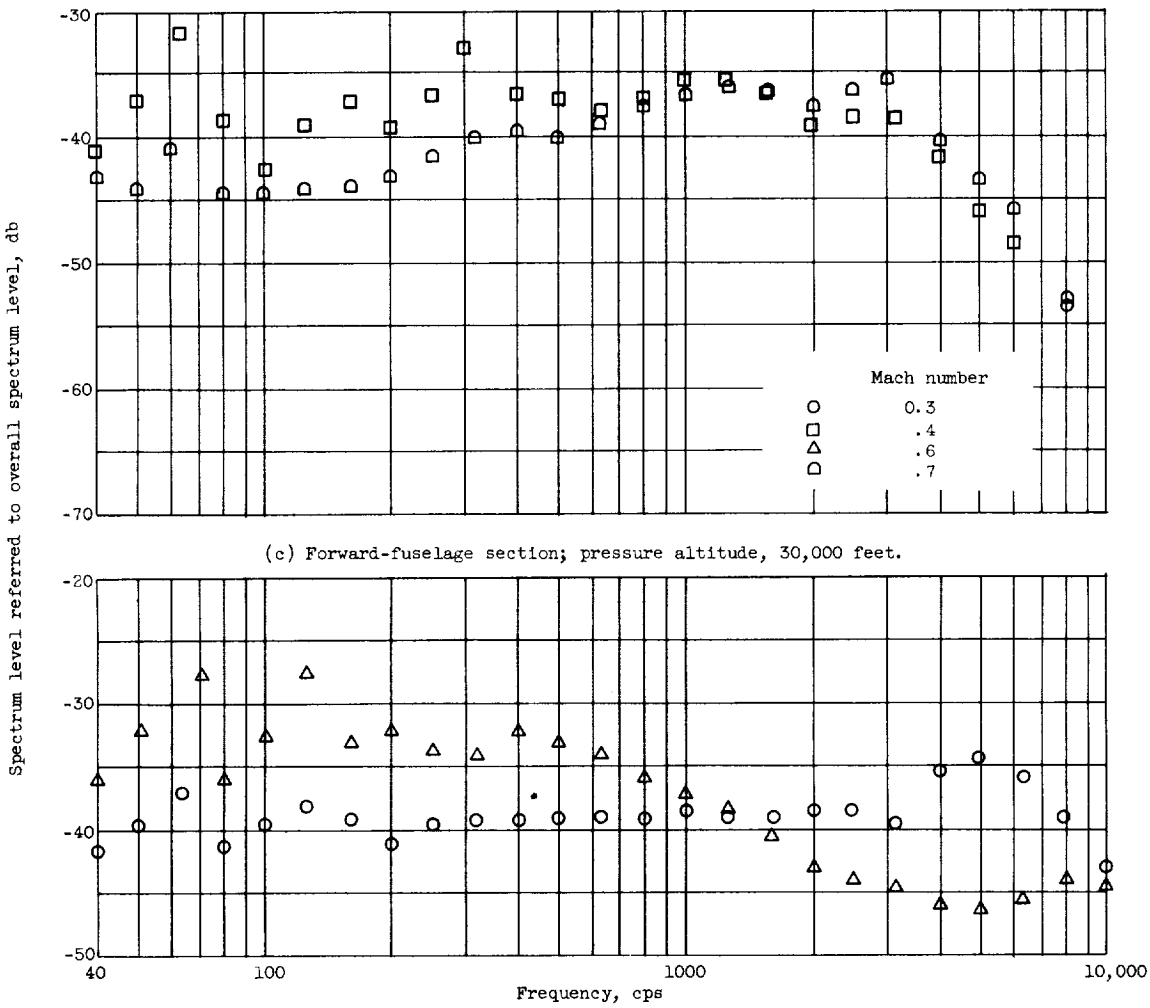

(c) Forward-fuselage section; pressure altitude, 30,000 feet.

(d) Wing; pressure altitude, 10,000 feet.

Figure 14. - Concluded. Wall-pressure spectrum level.

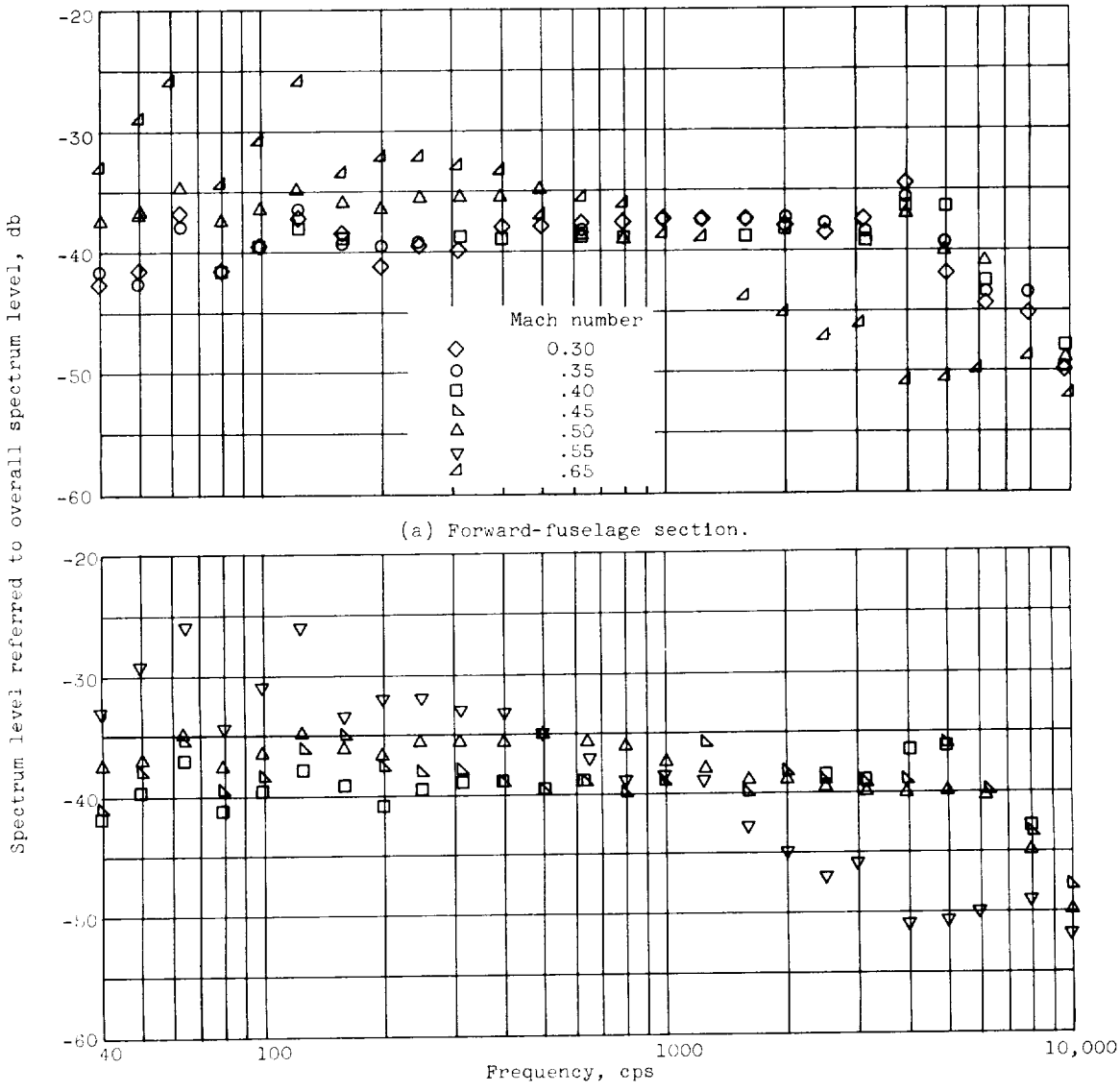

(a) Forward-fuselage section.

(b) Wing.

Figure 15. - Wall-pressure spectrum as function of Mach number. Pressure altitude, 10,000 feet.

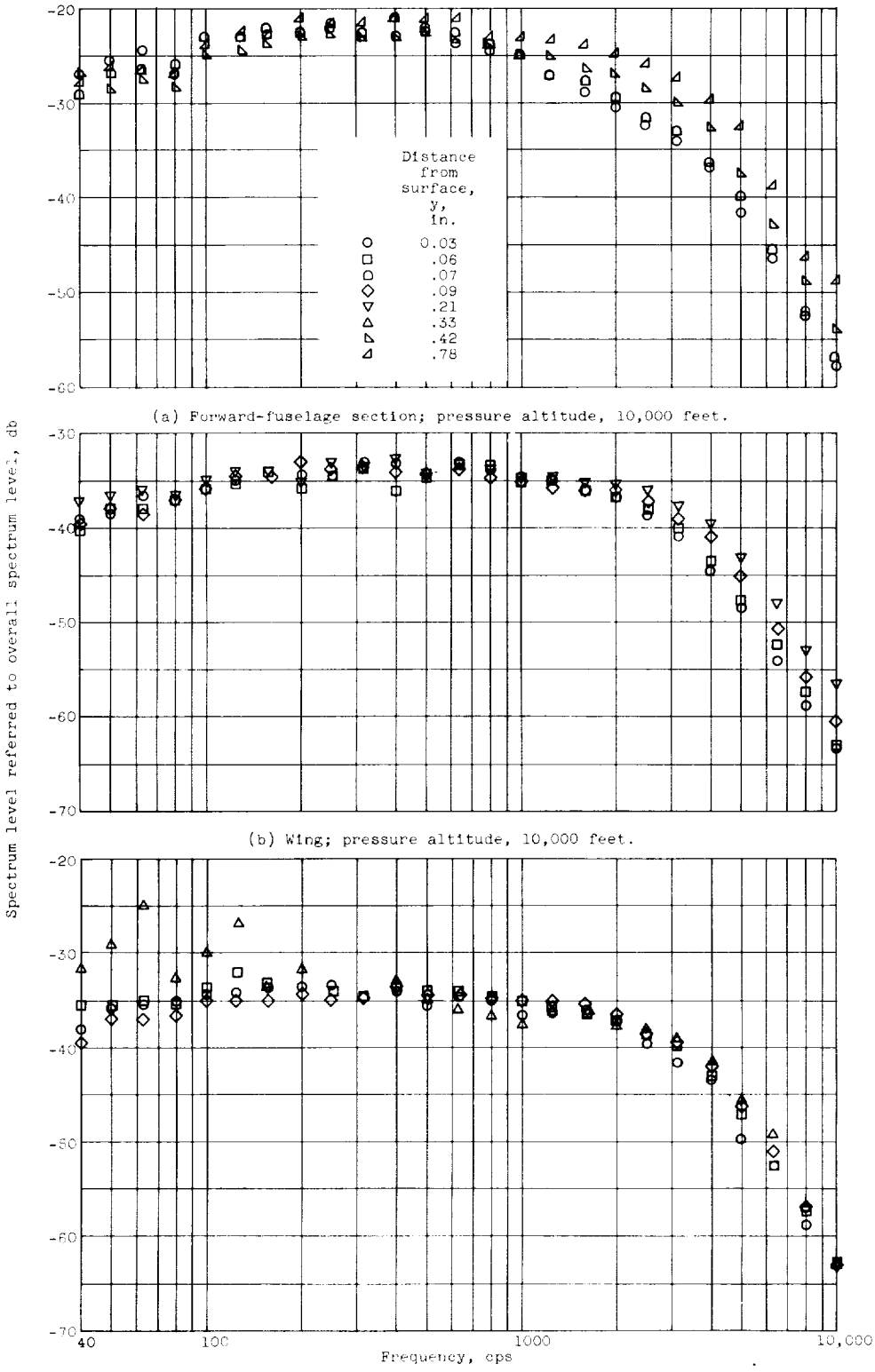

(a) Forward-fuselage section; pressure altitude, 10,000 feet.

(b) Wing; pressure altitude, 10,000 feet.

(c) Wing; pressure altitude, 20,000 feet.

Figure 16. - Boundary-layer longitudinal-velocity fluctuations.

E-911

NASA TN D-280
National Aeronautics and Space Administration.
FLIGHT MEASUREMENT OF WALL-PRESSURE FLUCTUATIONS AND BOUNDARY-LAYER TURBULENCE. Harold R. Mull and Joseph S. Algranti.
October 1960. 26p. OTS price, $0.75.
(NASA TECHNICAL NOTE D-280)

Boundary-layer velocity profiles, wall-pressure fluctuations, turbulence intensity, and associated spectral distributions for pressure altitudes of 10,000, 20,000, and 30,000 feet and for subsonic Mach numbers in the range 0.3 to 0.8 were measured at forward-fuselage and wing stations on a fighter-type jet aircraft. The measurements are in general agreement with results obtained in flight and in wind tunnels.

(Initial NASA distribution: 4, Aircraft safety and noise; 20, Fluid mechanics.)

Copies obtainable from NASA, Washington

I. Mull, Harold R.
II. Algranti, Joseph S.
III. NASA TN D-280

NASA

NASA TN D-280
National Aeronautics and Space Administration.
FLIGHT MEASUREMENT OF WALL-PRESSURE FLUCTUATIONS AND BOUNDARY-LAYER TURBULENCE. Harold R. Mull and Joseph S. Algranti.
October 1960. 26p. OTS price, $0.75.
(NASA TECHNICAL NOTE D-280)

Boundary-layer velocity profiles, wall-pressure fluctuations, turbulence intensity, and associated spectral distributions for pressure altitudes of 10,000, 20,000, and 30,000 feet and for subsonic Mach numbers in the range 0.3 to 0.8 were measured at forward-fuselage and wing stations on a fighter-type jet aircraft. The measurements are in general agreement with results obtained in flight and in wind tunnels.

(Initial NASA distribution: 4, Aircraft safety and noise; 20, Fluid mechanics.)

Copies obtainable from NASA, Washington

I. Mull, Harold R.
II. Algranti, Joseph S.
III. NASA TN D-280

NASA

NASA TN D-280
National Aeronautics and Space Administration.
FLIGHT MEASUREMENT OF WALL-PRESSURE FLUCTUATIONS AND BOUNDARY-LAYER TURBULENCE. Harold R. Mull and Joseph S. Algranti.
October 1960. 26p. OTS price, $0.75.
(NASA TECHNICAL NOTE D-280)

Boundary-layer velocity profiles, wall-pressure fluctuations, turbulence intensity, and associated spectral distributions for pressure altitudes of 10,000, 20,000, and 30,000 feet and for subsonic Mach numbers in the range 0.3 to 0.8 were measured at forward-fuselage and wing stations on a fighter-type jet aircraft. The measurements are in general agreement with results obtained in flight and in wind tunnels.

(Initial NASA distribution: 4, Aircraft safety and noise; 20, Fluid mechanics.)

Copies obtainable from NASA, Washington

I. Mull, Harold R.
II. Algranti, Joseph S.
III. NASA TN D-280

NASA

NASA TN D-280
National Aeronautics and Space Administration.
FLIGHT MEASUREMENT OF WALL-PRESSURE FLUCTUATIONS AND BOUNDARY-LAYER TURBULENCE. Harold R. Mull and Joseph S. Algranti.
October 1960. 26p. OTS price, $0.75.
(NASA TECHNICAL NOTE D-280)

Boundary-layer velocity profiles, wall-pressure fluctuations, turbulence intensity, and associated spectral distributions for pressure altitudes of 10,000, 20,000, and 30,000 feet and for subsonic Mach numbers in the range 0.3 to 0.8 were measured at forward-fuselage and wing stations on a fighter-type jet aircraft. The measurements are in general agreement with results obtained in flight and in wind tunnels.

(Initial NASA distribution: 4, Aircraft safety and noise; 20, Fluid mechanics.)

Copies obtainable from NASA, Washington

I. Mull, Harold R.
II. Algranti, Joseph S.
III. NASA TN D-280

NASA